Semiannual Progress Report

Submitted to:	National Aeronautics and Space Administration, Langley Research Center Hampton, Va 23665-5225 Atten: Dr. Robert C. Costen Technical Officer, MS / 493.
Institution:	Hampton University Dept. of Physics Hampton, Va 23668
Title of Research:	Direct Solar-Pumped Iodine Laser Amplifier
NASA Grant No:	NAG-1-441
Period Covered:	Sept. 1, 1988 -- Feb. 28, 1989
Principal Investigator: Co-Principal Investigator: Research Associate:	Kwang S. Han In Heon Hwang Larry V. Stock

Direct Solar-Pumped Iodine Laser Amplifier

Contents

Abstract

This Semiannual progress report covers the period from September 1, 1988 to February 28, 1989 under NASA grant NAG-1-441 entitled "Direct Solar-Pumped Iodine Laser Amplifier." During this period, the research effort was concentrated on the solar pumped master oscillator power amplifier (MOPA) system using n-C_3F_7I. In the experimental work, the amplification measurement was conducted to identify the optimum conditions for amplification of the center's Vortek solar simulator pumped iodine laser amplifier. A modeling effort was also pursued to explain the experimental results in the theoretical work. The amplification measurement of the solar simulator pumped iodine laser amplifier is the first amplification experiment on the continuously pumped amplifier. The small signal amplification of 5 was achieved for the triple pass geometry of the 15 cm long solar simulator pumped amplifier at the n-C_3F_7I pressure of 20 torr, at the flow velocity of 6 m/sec and at the pumping intensity of 1500 solar constants. The XeCl laser pumped iodine laser oscillator, which was developed in the previous research, was employed as the master oscillator for the amplification measurement.

In the theoretical work, the rate equations of the amplifier was established and the small signal amplification was calculated for the solar simulator pumped iodine laser amplifier. The amplification calculated from the kinetic equations with the previously measured rate coefficients reveals very large disagreement with experimental measurement. Moreover, the optimum condition predicted by the kinetic equation is quite discrepant with that measured by experiment. This fact indicates the necessity of study

in the measurement of rate coefficients of the continuously pumped iodine laser system.

I. Introduction

A space based solar pumped laser is a suitable energy source for the inter-planet space vehicles, for the transportation system on the moon and for the various rovers on the near Earth planets due to the long range transmission capability. However, the solar pumped laser research is on the fundamental stage and the suitable laser material is not yet found. Among the various laser materials proposed to be used in the solar pumped laser, only Nd:YAG [1] and the perfluoroalkyl iodide (such as C_3F_7I and C_4F_9I) [2,3] were successfully pumped by the solar radiation and the laser output power over 10 W could be obtained in the CW operation.

These two laser materials have advantages and disadvantages each other. The Nd:YAG is solid laser material so that the system could be rugged and the extractable power density is high compared with the gas material such as the perfluoroalkyl iodide. But it has a serious thermal distortion during continuous pumping and thus the heat removal from the laser material is a major issue.

On the contrary, the perfluoroalkyl iodides are gas media so that there is no thermal problem and the heat removal is relatively easy. However, the peak absorption wavelengths (~ 272 nm for C_3F_7I; ~ 286 nm for t-C_4F_9I) of the alkyl iodides are located at the far UV end of the solar spectrum and the absorption band is very narrow (~ 50 nm). Thus the utilization of the solar radiation is very low (~ 1 % for C_3F_7I: ~ 2 % for t-C_4F_9I) compared with Nd:YAG laser material (~ 14 %). Though the alkyl iodides are not suitable laser medium for the solar pumped laser due to the aforementioned disadvantages, the threshold pumping power could be reduced to about 100

solar constants [3] which suggests the simplicity of the solar collector.

A CW laser has the best applicability in space. However, the pulsed laser also may be suitable for certain application in space such as the laser propulsion of the space vehicles. Moreover, due to the weak solar irradiation (1.35 KW/m^2) on the earth surface, the amplifier scheme based on energy storage principle is more suitable for the development of the high power laser using laser materials with a long excited state lifetime such as iodine.

In this period of research, the amplification experiment was carried out by using a continuously solar simulator pumped iodine laser amplifier to study the energy storage capability of the iodine laser material. In the amplification measurement, the previously developed XeCl laser pumped iodine laser oscillator was employed as the master oscillator. At the same time, the theoretical calculation of the gain in the solar simulator pumped amplifier was performed to compare with the experimental results.

II. Solar Simulator Pumped Amplifier

The solar simulator used in this experiment is a vortex-stabilized continuous argon arc lamp (Vortek Industries Ltd.). This simulator can be operated with electrical power up to 100 KW. This solar simulator was employed in the CW iodine laser operation using n-C_3F_7I in the previous research [3]. The spectral irradiance on the amplifier tube surface was measured when an elliptic cylindrical reflector was used to focus the radiation emerging from the arc lamp into the amplifier tube. The measured spectral irradiance in the range from 200 nm to 400 nm was

almost equivalent to that of 1500 solar constant spectrum.

The experimental setup is shown in Fig. 1 for the measurement of the continuously pumped iodine laser amplifier by the solar simulator. The iodine laser oscillator was pumped by a XeCl laser developed in the previous research [4]. The iodine laser output was polarized by inserting two Brewster plates in the optical resonator of the iodine laser oscillatorthus the reflection from the windows of the amplifier could be minimized.

The pumped length of the amplifier tube by the solar simulator is only 15 cm and the inner diameter of the tube in 2 cm. The n-C_3F_7I gas in the amplifier tube is flowed at the speed in the range from 2 m/sec to 8 m/sec by adjusting the valves of the gas evaporator and the condenser. The flow velocity was monitored with a flowmeter (Hastings Flowmeter Model NALL-100 K).

As a first attempt, the amplification was measured at the pumping intensity of 1500 solar constants for the amplifier tube filled with 20 torr of n-C_3F_7I and with the flow velocity fixed at 7 m/sec. The laser energy input to the amplifier was 1 mJ with 0.5 cm in diameter when the laser oscillator was operated at 2 Hz but the input energy was reduced to 0.7 mJ when the laser oscillator was operated a 5 Hz due to the reduction of the XeCl pumping laser intensity. Thus the energy density of the input to the amplifier is 5.1 mJ/cm^2 when the laser is operated at 2 Hz, which is far less than the saturation energy density that is given by $E_S \cong h\nu / \sigma$ ($E_S \cong 22$ mJ/cm^2 for 20 torr of n-C_3F_7I). Therefore the amplification is in the small signal region.

The amplification result of the preliminary experiment is shown in Table 1. Here the amplification is defined as $\alpha = E_{out}/E_{in}$ and is denoted at

the bottom of the table.

Table I. Amplification by Solar Simulator Pumped Amplifier

		Oscillator operation frequency	
		2 Hz	5 Hz
Output energy	Without pumping amplifier	1.0 mJ	0.7 mJ
	With pumping amplifier	1.5 mJ	1.1 mJ
Amplification (α)	Experimental	1.5	1.57
	Theoretical (see III)	1.67	1.67

In the next step of experiment, the amplification was measured for the triple pass amplifier as shown in Fig. 2. This triple pass increases the gain length approximately three times compared with the single pass geometry. The experimental results are shown in Fig. 3 and Fig. 4. The maximum amplification was obtained at the flow velocity of about 6 m/sec and at the pressure of 20 torr for both 2 Hz and 5 Hz operations of the iodine laser oscillator. The maximum amplification obtained is about 5.

III. Theoretical Calculation of Amplification

To explain the experimental results, the amplification was evaluated theoretically in this research period. The most important quantity to be known is the density of the excited atomic iodine, [I*], for the evaluation of the amplification factor. To a good approximation, the excited atomic iodine density in the amplifier is governed by the following rate equation,

$$\frac{d[I^*]}{dt} = W_P [RI] - Q [RI] [I^*] - \frac{1}{\tau} [I^*] - k [R] [I^*] \qquad (1)$$

The first term in the right hand side represents the pumping rate (i.e. the photodissociation rate), the second term the quenching of the excited atomic iodine by the parent molecule, the third term the deexcitation by way of the spontaneous emission and the last term the recombination of the excited atomic iodine with the radical. The suitable approximations for the equation (1) to be solved analytically are (1) the density of the perfluoroalkyl iodide is constant during the pumping process because of the weak photodissociation rate (~ 1 %), (2) the radical density is equal to the excited atomic iodine density, (3) the lifetime of the excited atomic iodine is independent on the pressure. With these approximations, the differential equation (1) can be solved and the solution is given as

$$[I^*] = \frac{2c\,[1 - \exp(-\sqrt{b^2 + 4ac}\,t)]}{(\sqrt{b^2 + 4ac} + b) + (\sqrt{b^2 + 4ac} - b)\exp(-\sqrt{b^2 + 4ac}\,t)} \qquad (2)$$

where a = k, b = Q[RI] + $\frac{1}{\tau}$ and c = W_P [RI]. If we adopt the values k = 1 x 10^{-13} cm^3/sec [5], Q = 3 x 10^{-17} cm^3/sec [sec] [6], $\frac{1}{\tau}$ = 7.9 /sec and W_P [RI] = 3.12 x 10^{18} /sec as was calculated in the previous report [4], the excited atomic density is calculated from the equation (2) at various times. When the gas is flowed as in our experiment, the atomic excited iodine density varies along the axis of the amplifier tube. Thus the average excited atomic iodine contributes to the amplification. The average excited atomic iodine density calculated from the equation (2) is 5.7 x 10^{15} /cm^3 when the fill pressure is 20 torr and the flow velocity is 7 m/sec.

The small signal amplification α, which is defined as the ratio of the output energy density (J/cm^2) from the amplifier to the input energy density (J/cm^2), is given as

$$\alpha = \exp(\sigma N L) \qquad (3)$$

where σ is the stimulated emission cross section, N is the excited atomic iodine density and L is the length of the amplifier. The excited atomic iodine density to be substituted to equation (3) depends on the duration of the input laser pulse to the amplifier due to the finite relaxation time between the hyperfine levels of the excited state. In this experiment, the input pulse duration is about 25 nsec. Thus the total excited atomic iodine in the two hyperfine sublevels can contribute to the amplifier because the relaxation time in the hyperfine levels of the excited state is about 20 nsec [6]. Therefore the small signal amplification calculated from the equation (3) is 1.67 for the case of the single pass geometry. The stimulated

emission cross section adopted in this calculation is 6.0×10^{-18} cm^2 [7]. The amplification calculated for the triple pass amplifier is plotted in Fig. 3 and Fig. 4 with the experimental results.

IV. Kinetic Modeling of the Solar Simulator-Pumped Amplifier

The kinetic modeling effort has continued to identify the gain characteristics of the master oscillator power amplifier (MOPA) using the lasant n-C_3F_7I. These calculations are compared with the experimental results of a triple pass amplification, which was obtained at various gas pressures and flow velocities. In the calculation of the gain in the MOPA system, it is found that the output characteristics of the system are determined by the degree the molecular iodine increases inside the amplifier tube.

The kinetic model will be used to establish a scaling law for a solar-pumped iodine laser power generation system to be used for space-to-space power transmission.

A. Theoretical Considerations for the MOPA System

The gain coefficient before the input pulse is sent through the amplifying medium is calculated and the small signal gain is then calculated and compared to experimental results. Since the input energy density is very low compared with the saturation energy density, the small signal gain G_{SS} of the triple pass amplifier can be approximated by [8]

$$G_{ss} = \exp\{3\sigma \int_0^L ([I^*] - \tfrac{1}{2}[I])\, dz\}$$

where σ is the stimulated emission cross-section, L is the pumped length (15 cm) plus the downstream length (16.5 cm), and z represents the axial tube distance. The inversion density is given by ([I*]-1/2 [I]) and is a function of axial distance, which represents a maximum energy extraction efficiency. In reality, since the input pulse to the amplifier is about 25 ns, the energy extraction efficiency [9] is about 45%. The kinetic model used to find the gain is given below as a set of coupled nonlinear differential equations

$$d[RI]/dt = K_1 [R] [I^*] + K_2 [R] [I] - \xi_{RI} [RI] - K_4 [R] [RI] + K_5 [R] [I_2]$$

$$d[R]/dt = \xi_{RI} [RI] - K_1 [R] [I^*] - K_2 [R] [I] - 2 K_3 [R]^2 - K_4 [R] [RI] - K_5 [R] [I_2]$$

$$d[R_2]/dt = K_3 [R]^2 + K_4 [R] [RI]$$

$$d[I_2]/dt = C_1 [I] [I^*] [RI] + C_2 [I]^2 [RI] + C_3 [I] [I^*] [I_2] + C_4 [I]^2 [I_2] - \xi_{I2} [I_2] - K_5 [R] [I_2]$$

$$d[I^*]/dt = \xi_{RI} [RI] + \xi_{I2} [I_2] - K_1 [R] [I^*] - C_1 [I] [I^*] [RI] - C_3 [I] [I^*] [I_2] - Q_1 [I^*] [RI] - Q_2 [I^*] [I_2] - A [I^*] - [I^*]/\tau_D$$

$$d[I]/dt = \xi_{I2} [I_2] + Q_1 [I^*] [RI] + Q_2 [I^*] [I_2] + A [I^*] - C_1 [I] [I^*] [RI]$$

$$- 2\,C_2\,[I]^2\,[RI] - C_3\,[I]\,[I^*]\,[I_2] - 2\,C_4\,[I]^2\,[I_2] - K_2\,[R]\,[I]$$
$$+ K_4\,[R]\,[RI] + K_5\,[R]\,[I_2] - [I]/\tau_D$$

where ξ_{RI} and ξ_{I2} are the photodissociation rate for the parent molecule RI and molecular iodine I_2 respectively, A is the Einstein coefficient, and τ_D is the diffusion time constant [10]. The kinetic reaction rates [11] are given in Table II. It can be noted that the above differentials do not involve the photon density of the amplifier tube since the inversion is calculated before the amplified pulse is injected into the system. Expanding the above total differential to incorporate the flowing gas, the differential of the densities of the gas species $[x_i]$ become [11]

$$d[x_i]/dt = \partial[x_i]/\partial t + v\,\partial[x_i]/\partial z \quad i=1,2,\ldots,6$$

where the index i indicates the six gas species given above, and v=dz/dt is the flow rate in the z direction.

In the limit where the system reaches a steady state, the partial derivative with respect to time is zero and the set of differentials are solved as a function of z. It can be assumed that the system reaches a steady state between input pulses since the system operates between 2 to 5 Hz and is completely replenished between pulses. This calculation results in the gas densities given as a function of axial tube distance just before the oscillator pulse is injected into the cavity.

B. A Comparison of Theoretical Results with Experimental Data for the MOPA

An amplification experiment was preformed with a triple pass geometry varying the flow speed of the amplifying medium n-C_3F_7I for three pressures 10, 20, and 30 torr. The gain measured for this case is shown in figure 5 and compared with the theoretical calculations of the small signal gain G_{SS}. The peak gain was obtained experimentally at about 20 torr for a gas flow speed of about 7 m/s, but the maximum gain is calculated to be at about 2 m/s for a pressure of 10 torr. In addition, the calculation indicates a net absorption for 20 and 30 torr which would be due to I_2 buildup, and the absorption for 30 torr is greater than that of 20 torr for the same reason. In figure 6 the gain coefficient per unit distance for various flow velocities is given as a function of fill pressure. The peak gain is for a flow velocity of 1 m/s and a fill pressure of 13 torr. Figure 7 indicates the increase in a peak $[I_2]$ as a function of fill pressure. If a comparison between the maximum I_2 density and the gain coefficient is made, it can be seen that the increase in $[I_2]$ mitigates the inversion. Therefore, the inversion does not continue to increase as a function of pressure. On the other hand, as the flow velocity increases, the inversion does not increase as quickly.

In figures 8 through 13 the instantaneous gain coefficient $\sigma([I^*] - 1/2\,[I])$, the integrated gain coefficient

$$\sigma \int_0^Z ([I^*] - \tfrac{1}{2}[I])\, dz \,/\, L_C$$

and the molecular iodine density averaged over the distance of the tube, given as

$$L_C\,[I_2] \Big/ \int_0^{L_C} [I_2]\,dz$$

are plotted as a function of distance. Comparing flow velocities of 1 m/s and 2 m/s for a 11 torr fill pressure (figures 8 and 9), it can be seen that the slower production of [I*] allows $[I_2]$ to become dense enough to quench most of the gain in the pumped region of the amplifier. It is seen in figure 8 that after 15 cm, at which distance the amplifier is no longer illuminated, the inversion becomes insignificant; therefore, there is very little contribution to the gain after this distance. Here, for the maximum gain the inversion is positive throughout the pumped distance as apposed to figure 9 . In figures 10, 11, 12, and 13 the fill pressures are 10, 12, 13, and 14 torr respectively for a flow velocity of 1 m/s. From these four figures and figure 6, it can be seen that the $[I_2]$ does not significantly change the gain until 14 torr where the $[I_2]$ mediates the inversion inside the illuminated region of the amplifier tube. Figure 6 indicates the $[I_2]$ is not significant until about 12 torr for a flow velocity of 1 m/s. In this case the $[I_2]$ increases significantly because of the three body reactions given in Table II; they scale quadratically as the pressure of the amplifying medium increases.

V. Discussion

The experimental results shown in Table I is fairly well coincident with the theoretical calculation derived in the previous section. The experimental result measured for the triple pass geometry is also coincident with the theoretical consideration at the flow velocity of about 6 m/sec. However, the amplification measured in experiments at differnt flow velocities showes a drastic variation. The amplification decreases abruptly as the flow velocity recuces below 6 m/sec and also reduces abruptly as the flow velocity increases above 6 m/sec. The discrepancy between the theoretical calculation and the experimental result at the low flow velocity may originate from the ignorance of the quenching of the excited atomic iodine by the iodine molecule in the theoretical calculation. Really, in the course of experiment, the molecular iodine buildup was so serious that the amplification experiment could not be performed below the flow velocity of about 2.5 m/sec. However, the reduction in the amplification at the flow velocity above 6 m/sec is not explained with the molecular iodine quenching of the excited atomic iodine. Thus the main reason of the serious reduction at the high flow velocity is considered to be originated from the gas dynamic perturbation due to the gas flow.

The other point need to be mentioned is that the amplification measured at 20 torr of fill pressure is larger than the value of amplification measured at 30 torr. The theoretical calculation showes the higher amplification at 30 torr of fill pressure on the contrary to the experimental result. This fact indicates that the excited atomic iodine is more seriously quenched by the parent molecule when the pumping period is long.

Moreover the gas dymamic perturbation seems to contribute to the increase of the quenching rate.

The kinetic model calculation for the MOPA system has been carried out at the same time. The results of calculation is compared with the experimental data in Fig. 5. The theoretical result is rather contradictory to the experimental result. This indicates that some of the rate coefficients do not realistically explain the experimental results.

VI. Conclusion

The amplification of a continuously solar simulator pumped iodine laser amplifier has been measured for the first time in this research period. This experiment is a proof of the feasibility of the solar pumped iodine MOPA system. The small signal amplification of 5 was measured for triple pass of a 15 cm long amplifier with diameter 2 cm when n-C_3F_7I gas was flowed with 6 m/sec at the pressure of 20 torr. The optimum value of pressure times diameter of the amplifier is found to be 40 torr•cm for the solar simulator pumped amplifier which is far different from the case of the short pulse pumped high power iodine laser amplifier (P•d ≅ 150 torr•cm).

An analytical calculation for the amplification of the solar simulator pumped amplifier was carried out at the same time and the result was consistent with the experimentally measured peak amplification but the calculation could not explain the variation of amplification with the flow velocity of the n-C_3F_7I gas in the amplifier tube. A more precise kinetic model calculation was carried out in this period of research. However, the result of th calculation could not explain the experimental result and

moreover the calculation was rather contradictory to the experimental result. These discrepancy between the theoretical results and the experimental result seems to originate from the unsuitableness of the rate coefficients to this experiment and from the lack of understanding of the gas dynamic perurbation to the excited atomic iodine. Thus more concentrated research efforts on the kinetic study and on the gas dynamic effect are necessary in the future research.

References

[1] M. Weksler and J. Shwartz, IEEE J. Quant. Electron **24**, 1222 (1988) and references therein.

[2] J. H. Lee and W. R. Weaver, Appl. Phys. Lett. **39**, 137 (1981).

[3] J. H. Lee, M. H. Lee and W. R. Weaver, Proceedings of the International Conference on Lasers '86, p. 150, R. W. McMillan ed. STS Press, McLean, VA (1987).

[4] K. S. Han, I. H. Hwang and L. V. Stock, Semiannual Progress Report, NASA Grant NAG-1-441 (1988).

[5] S. V. Kuznetsova and A.I. Maslov, Sov. J. Quant. Electron **8**, 906 (1978).

[6] G. Brederlow, E. Fill and K. J. Witte, **The High-Power Iodine Laser**, Springer-Verlag, New York, N. Y. (1983), Chapter 2.

[7] K. Hola and K. L. Kompa, Handbook of Chemical Laser, ed. by R. W. F. Gross and J. F. Bott, John Wiley and Sons, New York, N. Y. (1986).

[8] L. M. Frantz and J. S Nodvik, "Theory of Pulse Propagation in a Laser Amplifier," J. of Appl. Phys., **34**, No. 8, August 1963.

[9] W. Fuss and K.L. Kompa: IPP Report, IPP IV / 67 (1967).

[10] J. W. Wilson, S. Raju, and Y. J. Shiu, "Solar-Simulator-Pumped Atomic Iodine Laser Kinetics, " NASA TP-2182, August 1983.

[11] John Heinbockel, NASA Progress Report of NAG-1-757, January 1988.

List of Figures

TABLE II - Reaction rate coefficients and their associated reactions for the lasant n-C_3F_7I along with the parameters used to modify the optical time constant.

Lasant Reactions	n-C_3F_7I Symbol	Reaction Rate Coefficient $(cm^3)^n/sec$
$R + I^* \rightarrow RI$	K_1	$.9000 \times 10^{-13}$
$R + I \rightarrow RI$	K_2	$.8050 \times 10^{-10}$
$R + R \rightarrow R_2$	K_3	$.2600 \times 10^{-11}$
$R + RI \rightarrow R_2 + I$	K_4	$.1000 \times 10^{-15}$
$R + I_2 \rightarrow RI + I$	K_5	$.3000 \times 10^{-10}$
$I^* + I + RI \rightarrow I_2 + RI$	C_1	$.1000 \times 10^{-32}$
$I + I + RI \rightarrow I_2 + RI$	C_2	$.3034 \times 10^{-30}$
$I^* + I + I_2 \rightarrow I_2 + I_2$	C_3	$.4440 \times 10^{-31}$
$I + I + I_2 \rightarrow I_2 + I_2$	C_4	$.3015 \times 10^{-29}$
$I^* + RI \rightarrow I + RI$	Q_1	$.4760 \times 10^{-16}$
$I^* + I_2 \rightarrow I + I_2$	Q_2	$.6587 \times 10^{-11}$
	T_s	.8700
	α	.0313

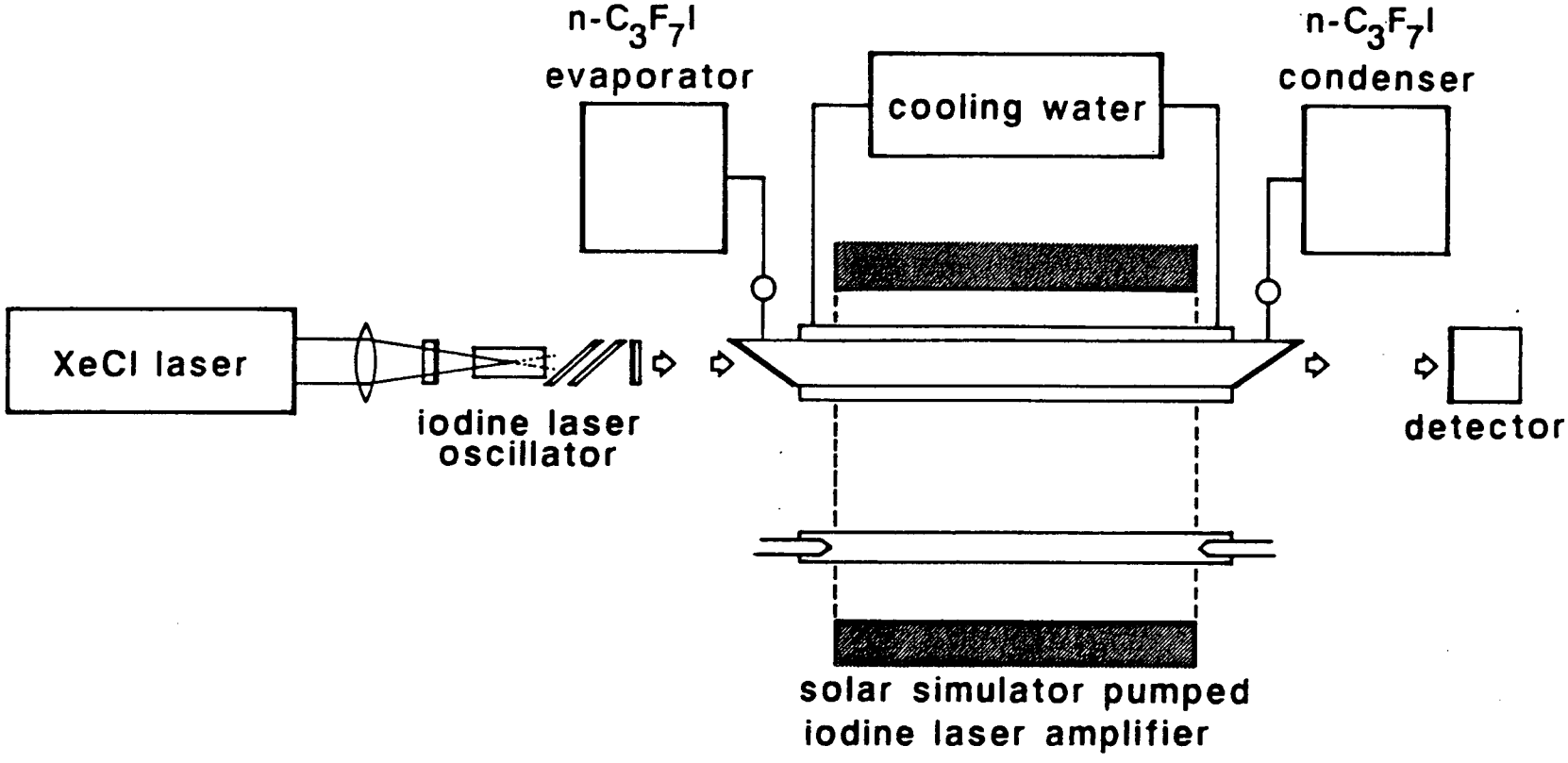

Fig. 1. Schematic diagram of the solar simulator pumped MOPA experiment.

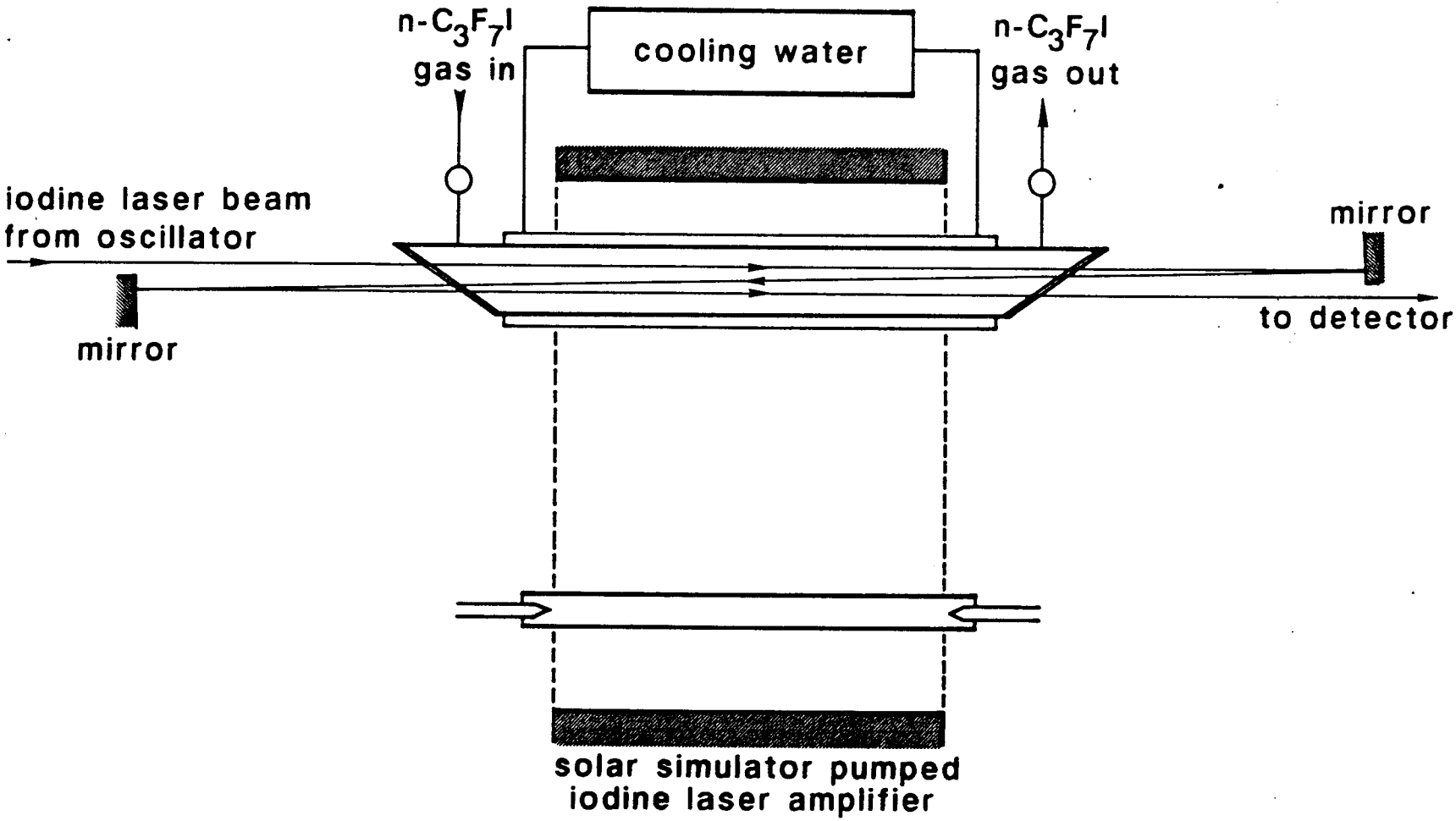

Fig. 2. Experimental arrangement for the measurement of the triple pass amplification by the solar simulator pumped amplifier.

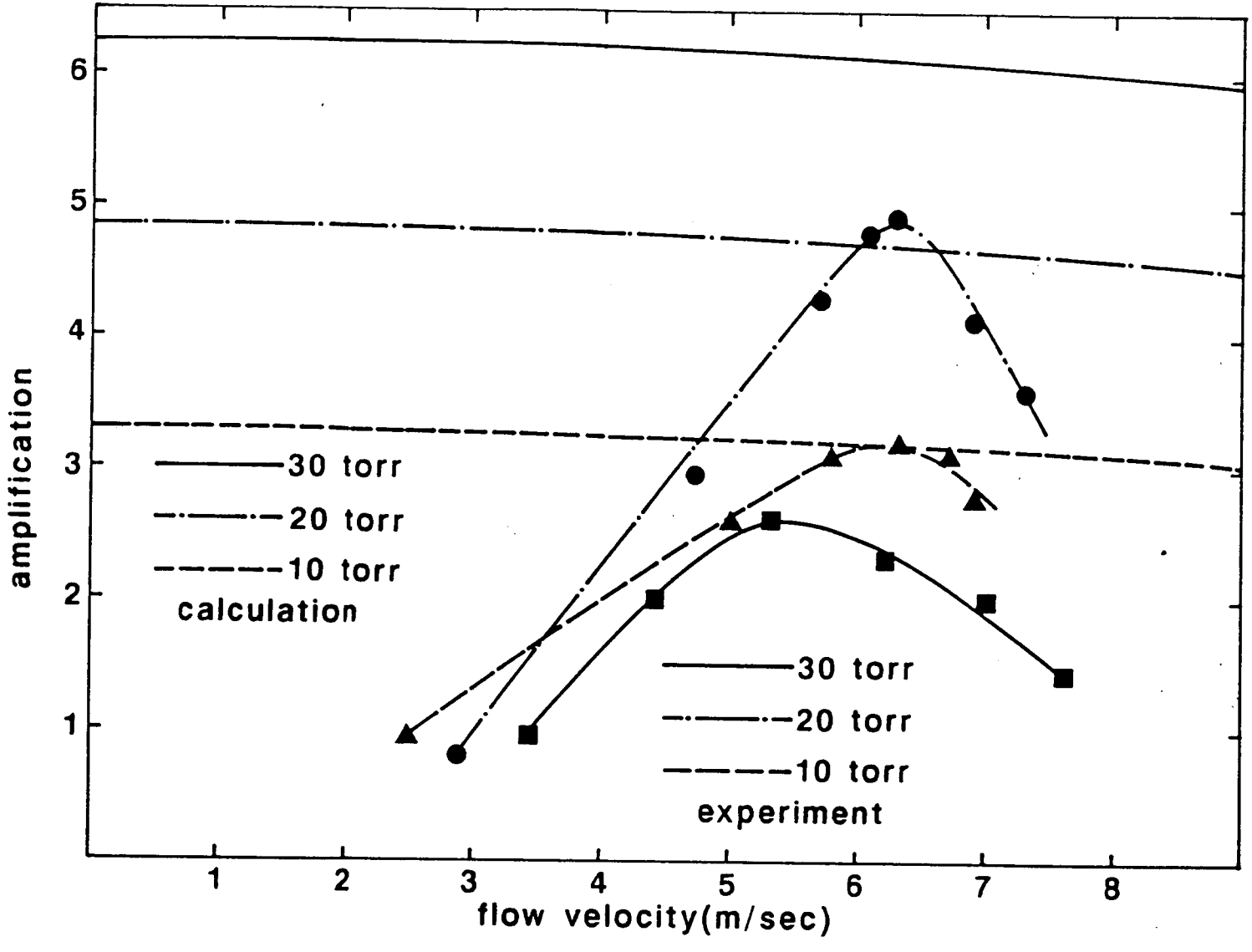

Fig. 3. Amplification measurement of the triple pass amplifier at different pressure and at different velocity of the n-C_3F_7I gas compared with the calculation at 2Hz operation (see text).

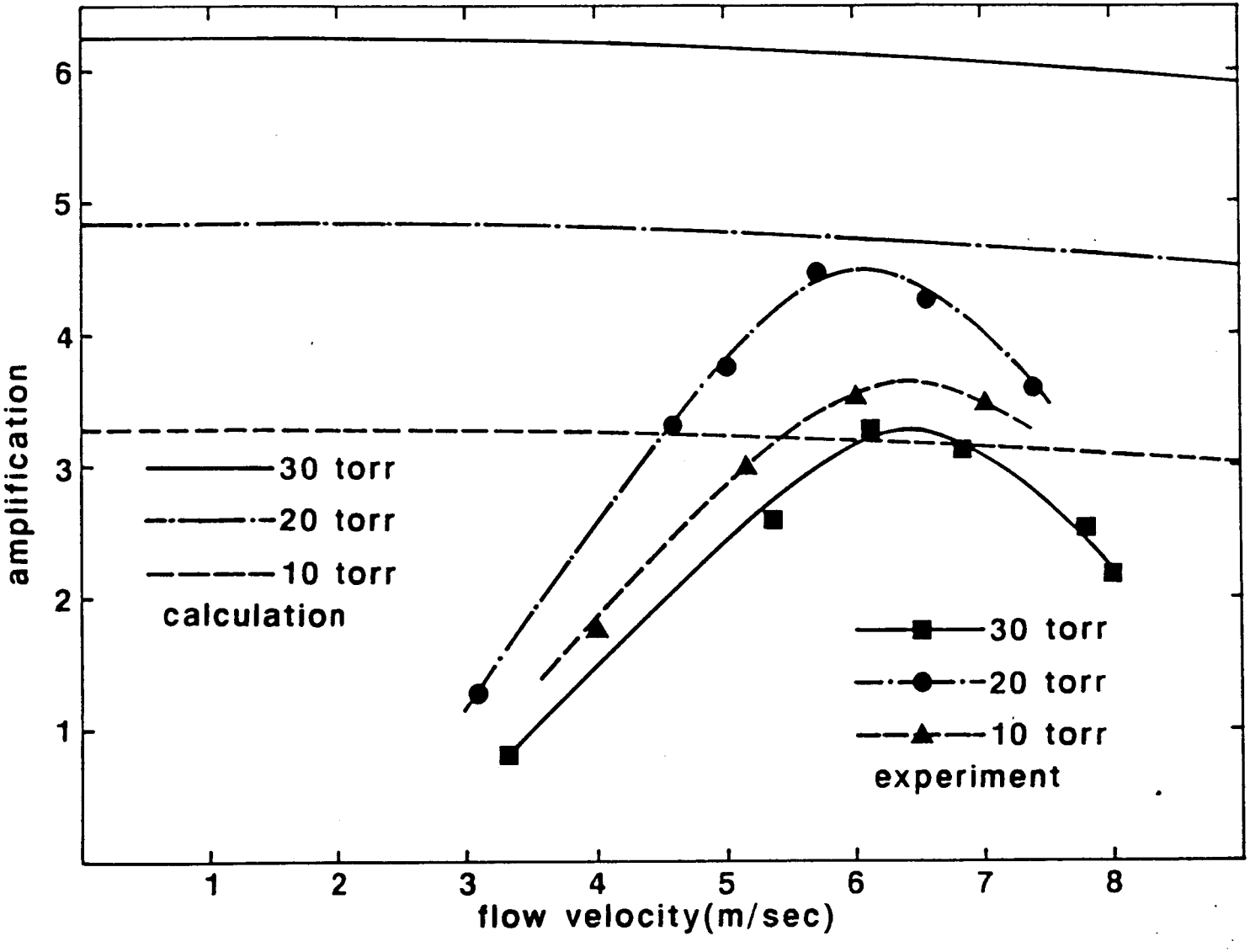

Fig. 4. Amplification measurement of the triple pass amplifier at different pressure and at different velocity of the n-C_3F_7I gas compared with the calculation at 5Hz operation (see text).

Theoretical Results and Experimental Data for the Triple-Pass Amplifier

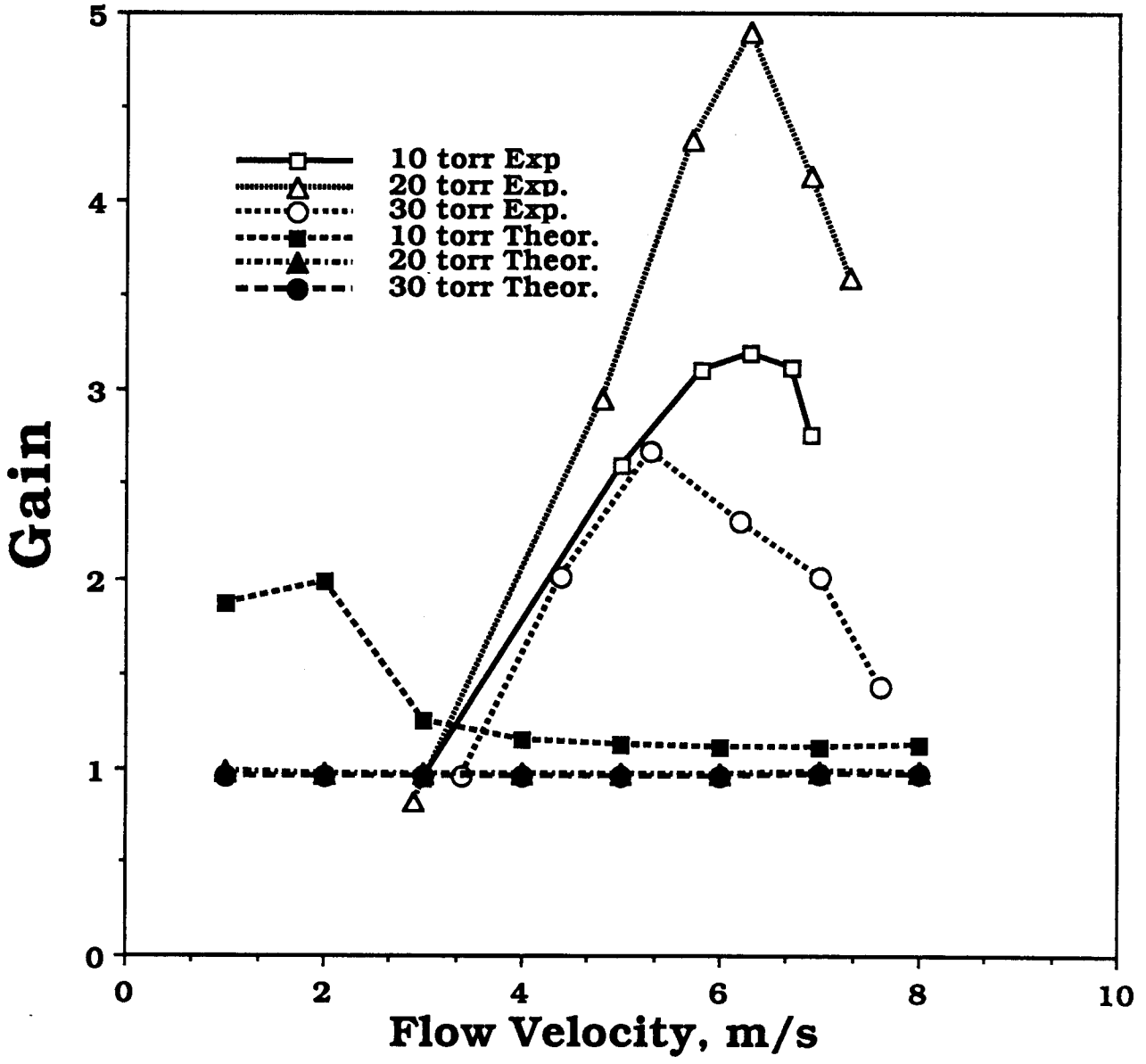

Figure 5.

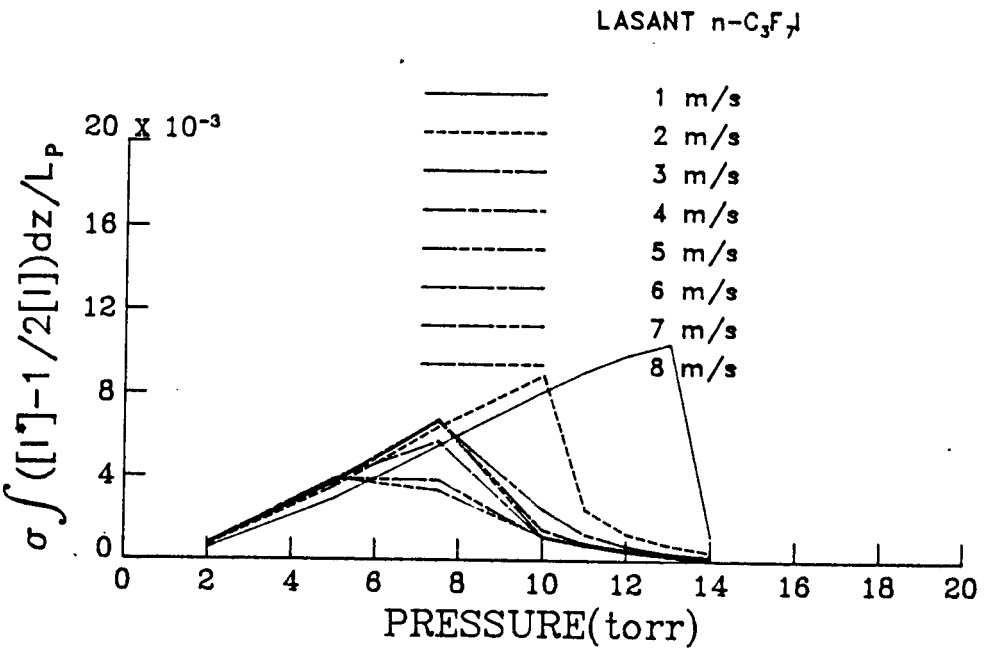

Figure 6.

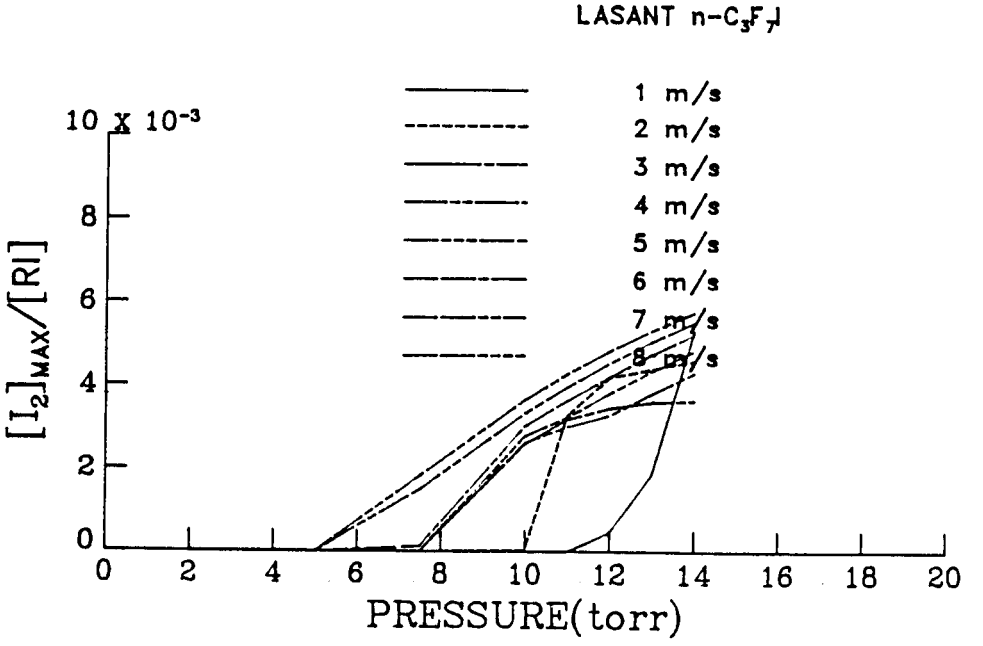

Figure 7.

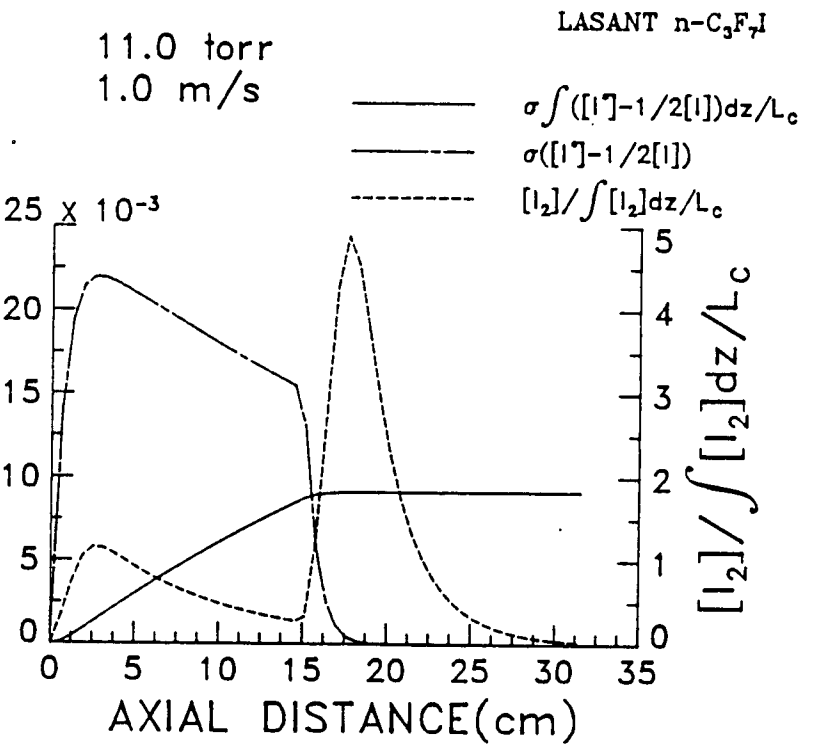

Figure 8.

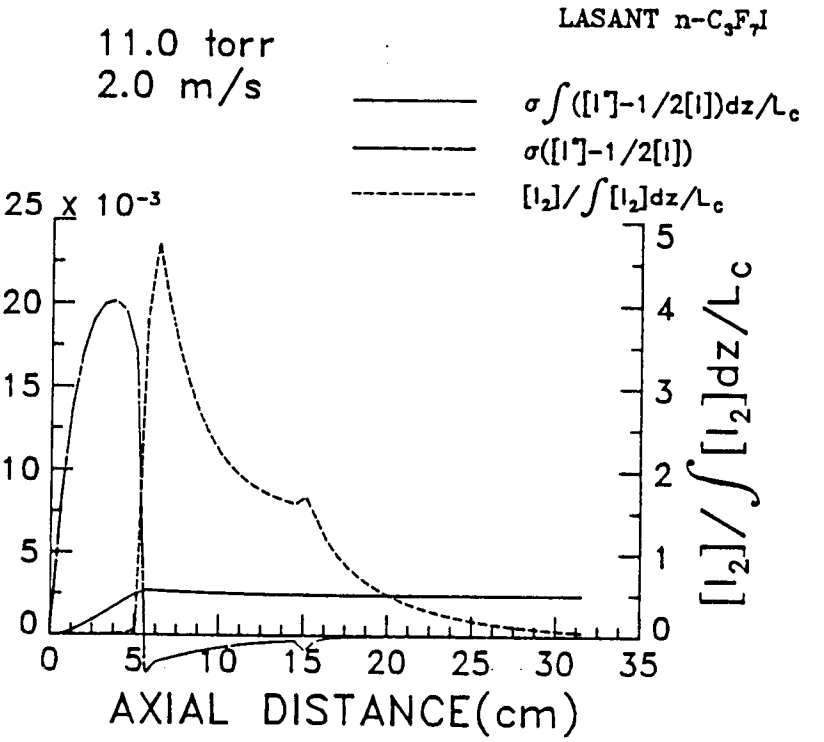

Figure 9.

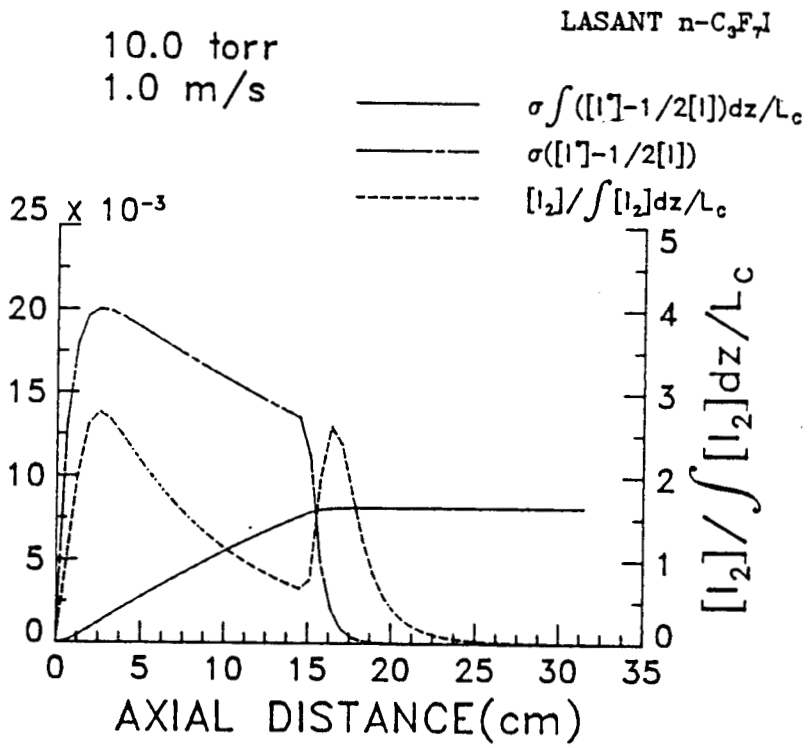

Figure 10.

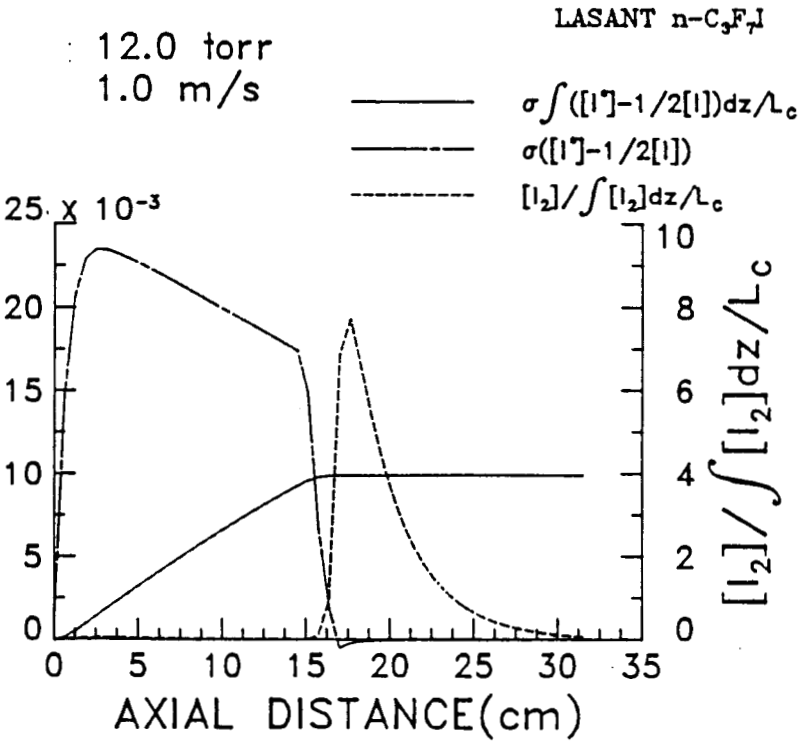

Figure 11.

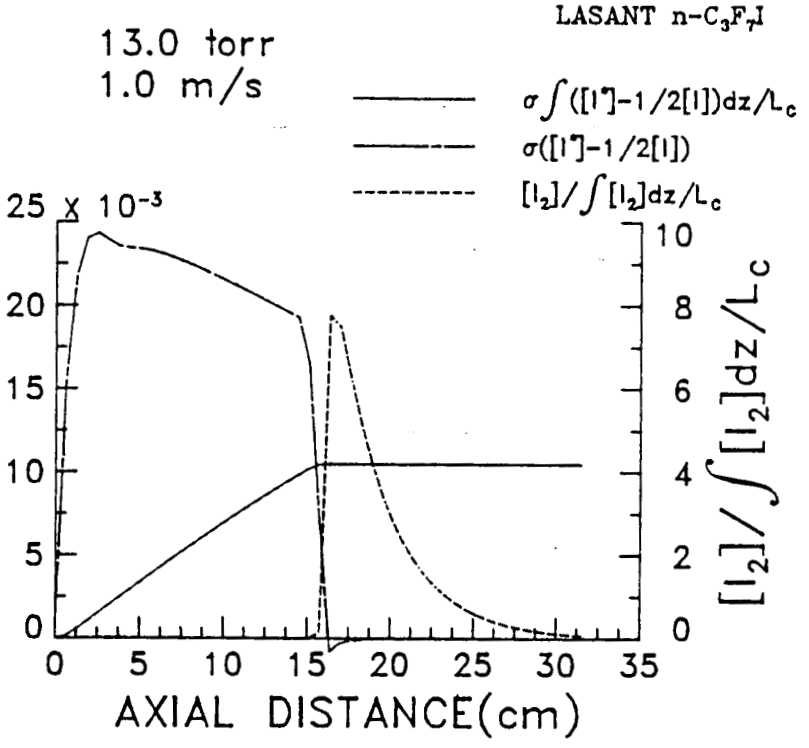

Figure 12.

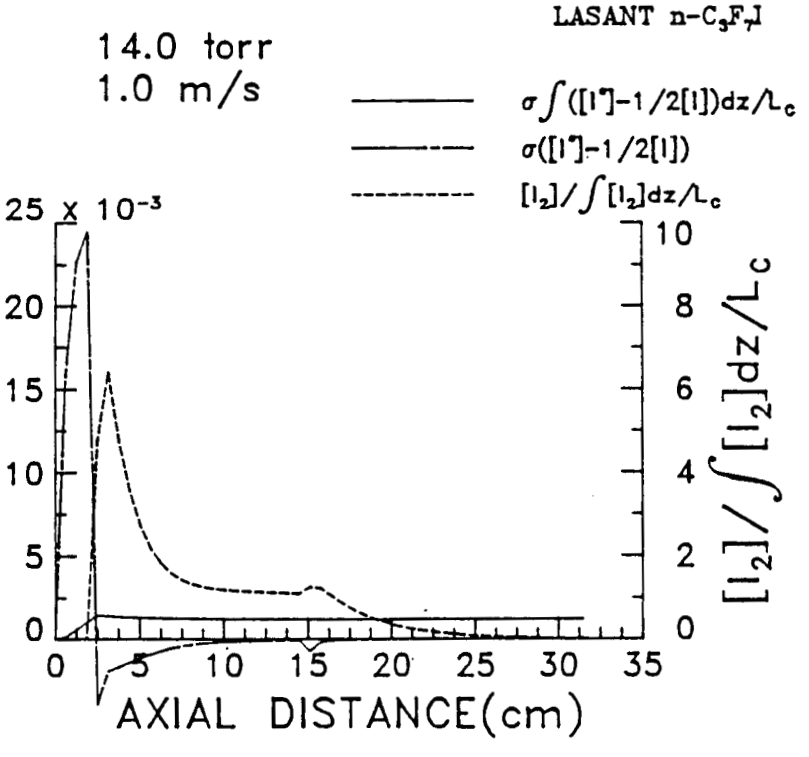

Figure 13.